Concurrent Computational and Dimensional Analyses of Design of Vehicle Floor-Plates for Landmine-Blast Survivability

M. Grujicic & B. A. Cheeseman

Journal of Materials Engineering and Performance

ISSN 1059-9495
Volume 23
Number 1

J. of Materi Eng and Perform (2014)
23:1-12
DOI 10.1007/s11665-013-0637-5

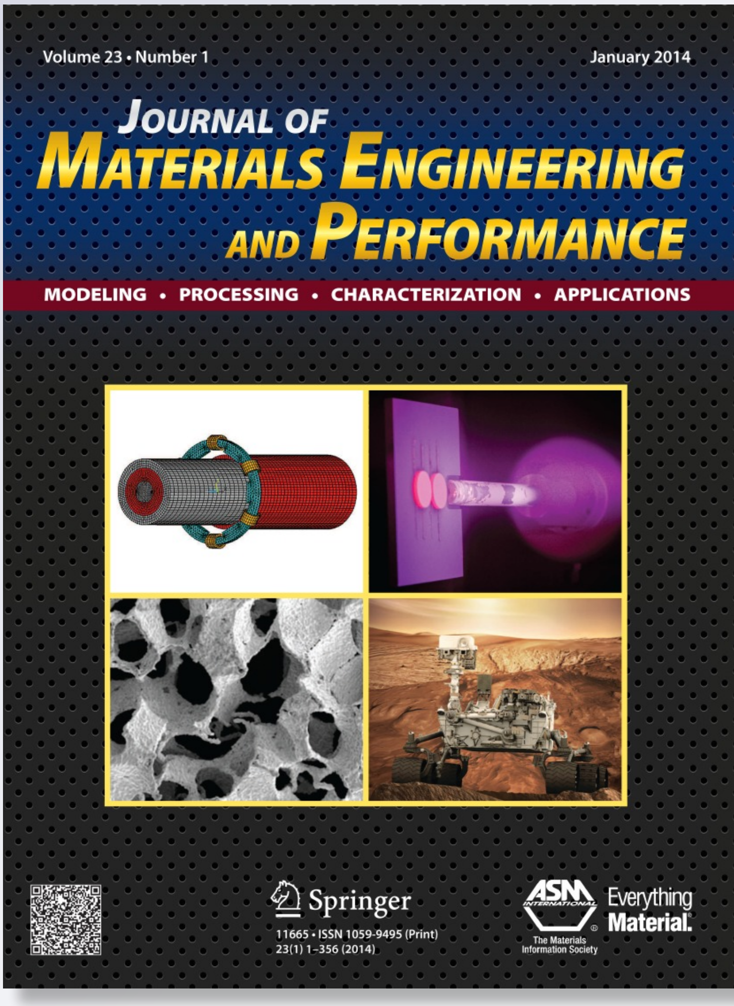

Report Documentation Page

Form Approved
OMB No. 0704-0188

1. REPORT DATE **2014**	2. REPORT TYPE	3. DATES COVERED **00-00-2014 to 00-00-2014**
4. TITLE AND SUBTITLE **Concurrent Computational and Dimensional Analyses of Design of Vehicle Floor-Plates for Landmine-Blast Survivability**		5a. CONTRACT NUMBER 5b. GRANT NUMBER 5c. PROGRAM ELEMENT NUMBER
6. AUTHOR(S)		5d. PROJECT NUMBER 5e. TASK NUMBER 5f. WORK UNIT NUMBER
7. PERFORMING ORGANIZATION NAME(S) AND ADDRESS(ES) **Clemson University,Department of Mechanical Engineering,241 Engineering Innovation Building,Clemson,SC,29634-0921**		8. PERFORMING ORGANIZATION REPORT NUMBER
9. SPONSORING/MONITORING AGENCY NAME(S) AND ADDRESS(ES)		10. SPONSOR/MONITOR’S ACRONYM(S) 11. SPONSOR/MONITOR’S REPORT NUMBER(S)
12. DISTRIBUTION/AVAILABILITY STATEMENT **Approved for public release; distribution unlimited**		
13. SUPPLEMENTARY NOTES		
14. ABSTRACT		
15. SUBJECT TERMS		

16. SECURITY CLASSIFICATION OF:			17. LIMITATION OF ABSTRACT	18. NUMBER OF PAGES	19a. NAME OF RESPONSIBLE PERSON
a. REPORT **unclassified**	b. ABSTRACT **unclassified**	c. THIS PAGE **unclassified**	**Same as Report (SAR)**	**14**	

Standard Form 298 (Rev. 8-98)
Prescribed by ANSI Std Z39-18

JMEPEG (2014) 23:1–12
DOI: 10.1007/s11665-013-0637-5

1059-9495/$19.00

Concurrent Computational and Dimensional Analyses of Design of Vehicle Floor-Plates for Landmine-Blast Survivability

M. Grujicic and B.A. Cheeseman

(Submitted January 3, 2013; published online August 9, 2013)

Development of military vehicles capable of surviving landmine blast is seldom done using full-scale prototype testing because of the associated prohibitively-high cost, the destructive nature of testing, and the requirements for major large-scale experimental-test facilities and a large crew of engineers committed to the task. Instead, tests of small-scale models are generally employed and the model-based results are scaled up to the full-size vehicle. In these scale-up efforts, various dimensional analyses are used whose establishment and validation requires major experimental testing efforts and different-scale models. In the present work, an approach is proposed within which concurrent and interactive applications of the computational analyses (of landmine detonation and the interaction of detonation products and soil ejecta with the vehicle hull-floor) and the corresponding dimensional analysis are utilized. It is argued that this approach can guide the design of military-vehicle hull-floors which provide the required level of protection to the vehicle occupants under landmine blast attack without introducing unnecessarily high weight to the vehicle. To validate this approach, a combined Eulerian/Lagrangian formulation for landmine detonation and the interaction of detonation products and soil ejecta with the vehicle hull-floor (developed in our previous work) has been utilized along with the experimental results pertaining to small-scale model and full-scale vehicle testing.

Keywords dimensional analysis, landmine detonation, vehicle hull-floor design

1. Introduction

Recent efforts of the U. S. Army have been aimed at becoming more mobile, deployable, and sustainable while maintaining or surpassing the current levels of lethality and survivability. Current battlefield vehicles have reached in excess of 70 tons due to ever increasing lethality of ballistic threats which hinders their ability to be readily transported and sustained. Therefore, a number of research and development programs are under way to engineer light-weight, highly mobile, transportable, and lethal battlefield vehicles with a target weight under 20 tons. To attain these goals, significant advances are needed in the areas of light-weight materials and structures as well as in the areas of computer-aided design and experimental testing/validation techniques for these vehicles.

Over the last two decades, the use of computational analyses in the design of military vehicles has continuously increased. Efficient computational codes and fast, massive, and inexpensive computational resources enable today computational investigations of whole-vehicle performance under various in-service (Ref 1) and threat (Ref 2-4) conditions. However, the true utility of these computational analyses remains questionable considering that critical shortcomings of these analyses, are either not fully identified or understood. For example, material models used in these analyses need substantial improvements to take into account the contribution of various microstructural effects (at various length scales), the effects of components manufacturing and assembly as well as the effects of realistic environmental, thermal, mechanical, and dynamic loading conditions on material behavior (Ref 5). In addition, many issues associated with the interactions and contacts between the vehicle and its surrounding (including fluid/liquid interactions) are still not fully resolved. This situation requires that extensive experimental testing and validation efforts still be employed during development of new or retro fitting of the existing military vehicles. In other words, computational analyses are presently capable of reducing somewhat the new-vehicle development time and of lowering the extent of (but not fully eliminating a need for) the experimental testing and validation efforts.

The main issue with the experimental testing/validation efforts is that they should ideally involve full-scale prototypes of the vehicles, which is quite expensive and requires major test facilities and a large crew of engineers committed to the task. On the other hand, it is quite advantageous to carry out all the experimental testing and validation using small-scale models and to then scale-up the model results to the full-scale prototype, using the appropriate dimensional analysis (defined later). In trying to attain this goal, computational analyses can play a critical role. That is, the computational analyses can be

M. Grujicic, Department of Mechanical Engineering, Clemson University, 241 Engineering Innovation Building, Clemson, SC 29634-0921; and **B.A. Cheeseman**, Army Research Laboratory—Survivability Materials Branch, Aberdeen Proving Ground, MD 21005-5069. Contact e-mail: gmica@clemson.edu.

first validated experimentally using a single small-scale model. Then, the computational analyses can be employed to establish the basic fundamental parameters and their inter-relations and, in turn to develop the appropriate dimensional analysis. This could potentially lead to significant reductions in the small scale model testing efforts (e.g., different-scale models would not have to be employed to establish/validate the dimensional analysis). Lastly, both the computational and experimental model scale-up predictions can be used, with more confidence, in the design/development of full-scale prototypes.

A review of the public-domain literature carried out as part of the present work revealed that the landmine-detonation related research activities can be broadly divided into three main categories: (a) shock and blast wave mechanics/dynamics including landmine-detonation phenomena and large-deformation/high-deformation rate constitutive models for the attendant materials (high explosive, air, soil, etc.) (Ref 6); (b) the kinematic and structural response of the target to blast loading including the role of target design and use of blast attenuation materials (Ref 7); and (c) vulnerability of human beings to post-detonation phenomena such as high blast pressures, spall fragments, and large vertical and lateral accelerations (Ref 2). The present work falls into the categories (a) and (b) of the research listed above since it emphasizes both the role of material behavior under transient-dynamic loading conditions as well as the kinematic and structural responses of the target structure to detonation of landmines shallow buried in soil.

The main objective of the present work is to extend the scaling analysis of Wenzel and Hennessey (Ref 8) for military vehicle-hull floor-plates subjected to impulse and high-pressure loads associated with detonation of a landmine buried in soil under the hull body. The dimensional analysis of Wenzel and Hennessey (Ref 8) is based on the so-called Buckingham Theorem (Ref 9), a procedure commonly used in the situations in which full-scale structures/prototypes are designed and sized based on the results obtained using small-scale model tests. To extend the dimensional analysis of Wenzel and Hennessey (Ref 8), the combined Eulerian/Lagrangian computational model and analysis of detonation of landmines shallow-buried in soil and of the interactions between detonation products and soil ejecta with the target structure developed by Grujicic et al. (Ref 10) is used.

The main role of the military-vehicle hull-floor is to protect the vehicle occupants in the case of detonation of a landmine buried in soil underneath the vehicle belly. Complex interrelationships generally exist between the type and the extent of vehicle-occupants injuries and the extent of vehicle damage resulting from under-the-vehicle landmine blast. The most serious vehicle-occupants injuries and their fatalities are most frequently incurred as a consequence of hull-floor rupture. In addition to generating floor-material fragmentation, floor rupture enables for the ingress of flame and toxic (detonation-product) gases and can lead to on-board fires and explosions. While the vehicle under landmine attack is always subjected to high "G") forces, this aspect of the threat is usually considered as secondary when floor rupture takes place. On the other hand, when landmine-detonation results in only hull-floor bulging, the vehicle is then propelled upward and off the ground, to an extent which scales directly with size of the landmine and inversely with vehicle weight. The accompanying dynamic shock can cause vehicle occupants and on-board instruments and weapons to be thrown about within the vehicle interior. In addition, large hull-floor deflections and deformations can cause a sequence of failures throughout the entire vehicle through components/sub-system connections and interfaces (e.g., via fuel lines running along the floor, floor-bolted seats, ammunition storage racks, power-train lines, etc.). Traditionally, the floor-rupture problem is solved through the use of thicker floor-plates, stronger, tougher, and usually heavier material and through the utilization of applique armor. This approach is generally associated with unnecessary oversized/overweight vehicle-hull floors and, is being abandoned nowadays due to aforementioned military's requirements for lighter vehicles. Combined application of the computational analyses of both small-scale models and full-scale prototypes of vehicles (or their hulls) subjected to landmine blast and a dimensional analysis for model-results scale-up, proposed in the present work, is a way to reduce the weight of the vehicles while ensuring the required confidence level for its survivability and survivability of its occupants.

The organization of the paper is as follows: In section 2.1, a brief overview is provided of the Buckingham Π theorem (Ref 9). The dimensional analysis for military-vehicle floor-plates subjected to landmine-detonation attack originally proposed by Wenzel and Hennessey (Ref 8) is overviewed in section 2.2. The combined Eulerian/Lagrangian computational procedure used in the present work is described in section 2. The main results obtained in the present work are presented and discussed in section 3, while the key conclusions resulted from the present study are summarized in section 4.

2. Computational Procedure

2.1 Buckingham Π Theorem (Ref 9)

As discussed earlier, the Buckingham Π theorem (also known as the "similitude theory") (Ref 9) is employed in the present work to address the problem of computational-analysis validation via small-scale model testing and the problem of scale-up of the model results to the full-scale prototype. In the remainder of this section, a brief overview is provided of the similitude theory and of its utility and limitations.

The similitude theory (also known as the "dimensional analysis") is essentially a technique/procedure for describing the behavior of a system in terms of a number of dimensionless parameters (generally referred to as the Π terms). This procedure typically involves the following main steps:

(a) Identification of all physical parameters which govern the behavior of the system under investigation. This is the most critical step in the dimensional analysis since it requires a good understanding of the underlying physics of the problem at hand (even in the case when the functional forms of the governing equations are not known).
(b) Specification of the units for the physical parameters defined in (a) in terms of the fundamental physical dimensions (typically force, length, and time).
(c) Identification of a subset of parameters among the physical parameters defined in (a) with the number of parameters in this subset being equal to the number of fundamental physical dimensions defined in (b). The parameters in this subset will be used for converting the remaining parameters in (a) into a set of dimensionless parameters (i.e., the Π terms). It should be noted that while the number of the resulting Π terms is fully

defined (equal to the number of physical parameters in (a) minus the number of fundamental dimensions in (b)), the functional form of the Π terms is not unique. It is generally advantageous to define the Π terms in such a way that they have a clear physical meaning. However, regardless of the choice of the Π terms, the final implications/findings offered by the similitude theory is independent of this choice (provided, all the governing physical parameters are correctly identified in (a)).

(d) Identification of the functional relationships between each of the Π terms and all other Π terms. These relations are generally determined using experimental or computational approaches or the combination of the two approaches.

The power of the similitude theory is that the functional relations offered are generalized, i.e., the effect of geometrical, kinematic, ambient, loading, and response scales is eliminated. Consequently, the similitude theory states that, if all the pertinent physical parameters were correctly identified in (a) and if all the Π terms were kept invariant (i.e. unchanged) between a small-scale model and its full-scale prototype, then the results obtained using a small-scale model could be directly used to predict the response of the corresponding full-scale counterpart.

2.2 Brief Overview of the Wenzel and Hennessey Work (Ref 8)

As mentioned earlier, one of the main objectives of the present work is to further advance the dimensional analysis presented by Wenzel and Hennessey (Ref 8). In the remainder of the section, a brief overview is provided of this work.

The work of Wenzel and Hennessey (Ref 8) deals with scaling floor-plates for military vehicles expected to be targeted by landmine blast. The main objective of the work was to develop and validate a dimensional analysis for the vehicle floor-plate sizing problem, so that the results of small-scale replica-model can be used to determine the minimal required floor-plate thickness which will ensure that, under the specific landmine-detonation scenario, the vehicle floor will not undergo rupture or extensive dynamic deflection. The term "replica-model" will be defined in greater detail later in this section. Until then, this term will be used to denote a small-scale model which is similar (geometrically, constitutively, and with respect to extent of properly scaled loads and structural responses) to the corresponding full-scale prototype.

The starting point in the work of Wenzel and Hennessey (Ref 8) was to take advantage of the fact that floor-plate deflections do not significantly modify the (landmine-detonation-induced) dynamic loading. Toward that end, the problem at hand was divided (decoupled) in two separate problems: (a) a floor-plate structural response problem and (b) the problem of analyzing pressures and impulses resulting from detonation of a landmine (shallow buried in soil underneath the vehicle-hull bottom).

2.2.1 Structural Response. *Physical Parameters.* By carrying out a careful and detailed engineering analysis of the structural response of a thick metal plate (a model for the vehicle-hull bottom) supported on wooden blocks (to obtain the required level of ground clearance), and clamped along its edges (to simulate the effect of the surrounding/supported vehicle-frame structure), Fig. 1, Wenzel and Hennessey (Ref 8) identified eleven key physical parameters which govern the response of the plate subjected to landmine-detonation loading. These parameters are listed and explained and their fundamental dimensions are identified in Table 1.

Π *Terms.* Next, three of the physical parameters listed in Table 1 (floor-plate thickness, h, floor-plate material yield strength, σ, and the same material density, ρ) are used for constructing eight Π terms (Table 2).

It should be noted that the rigid body motion of the floor-plate was neglected due to the fact that it did not modify landmine-detonation-induced loading and, hence, did not modify the structural response of the floor-plate. The distributed inertial effects, on the other hand, were included through the selection of the material density and the floor-plate thickness. It should be also noted that no explicit consideration of the effect of change in the strain rates was considered with a justification that the strain rates do not appreciably change between the full-scale prototype and its replica-model. However, it should be recognized that the effect of high strain rates was included implicitly, via the use of the dynamic material yield strength, σ.

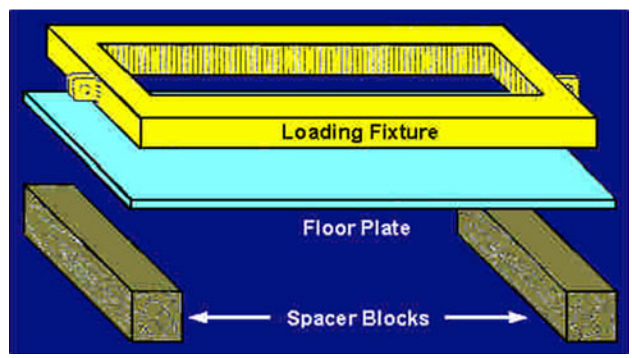

Fig. 1 A schematic of the prototype landmine-blast test set-up used in the work of Wenzel and Hennessey (Ref 8)

Table 1 Key physical parameters controlling structural response of the vehicle-floor plates

Symbol	Parameter	Fundamental dimensions
P	Pressure due to landmine detonation	F/L^2
I	Specific impulse due to landmine detonation	FT/L^2
h	Floor-plate thickness	L
h_i	Array of other (non-dimensional) floor-plate dimensions	…
σ	Floor-plate material yield strength	F/L^2
σ_i	Array of other (non-dimensional) strength parameters for floor-plate material	…
ε	Floor-plate material equivalent strain	…
ρ	Floor-plate material density	FT^2/L^4
δ	Floor-plate deflection	L
a	Floor-plate acceleration	L/T^2
t	Post landmine-detonation time	T

Table 2 Π terms controlling structural response of the vehicle-floor plates

Π term	Physical meaning	Similarity type
$\Pi_1 = h_i$	Array of non-thickness (non-dimensional) floor-plate dimensions	Geometrical
$\Pi_2 = \sigma_i$	Array of non-yield-strength (non-dimensional) parameters for floor-plate material	Constitutive
$\Pi_3 = \varepsilon$	Floor-plate material equivalent strain	Constitutive, response
$\Pi_4 = \delta/h$	Thickness-scaled floor-plate deflection	Response
$\Pi_5 = a\rho h/\sigma$	Non-dimensional floor-plate acceleration	Response
$\Pi_6 = (t\sigma^{1/2})/(h\rho^{1/2})$	Non-dimensional time	Response
$\Pi_7 = I/(\sigma^{1/2}\rho^{1/2}h)$	Non-dimensional impulse due to landmine detonation	Loading
$\Pi_8 = P/\sigma$	Non-dimensional pressure due to landmine detonation	Loading

Table 3 Replica-to-prototype scaling for structural response of the vehicle-floor plates

Symbol	Parameter	Scale factor
h_i	Array of non-thickness (non-dimensional) floor-plate dimensions	λ
ρ	Floor-plate material density	1.0
σ	Floor-plate material yield strength	1.0
ε	Floor-plate material equivalent strain	1.0
δ	Floor-plate deflection	λ
a	Floor-plate acceleration	$1/\lambda$
t	Post landmine-detonation time	λ
I	Specific impulse due to landmine detonation	λ
P	Pressure due to landmine detonation	1.0

Scaling. As mentioned earlier, in accordance with the similitude theory, for the results obtained using small-scale model to be applicable at the prototype scale, the Π terms must be unchanged between the model and the prototype. In order to ensure this condition, the model and the prototype must be similar geometrically, (i.e., Π_1 is unchanged), constitutively (i.e., Π_2 and Π_3 terms are unchanged), in response (i.e., Π_3-Π_6 terms are unchanged) and with respect to loading (Π_7 and Π_8 terms are unchanged). Hence, if the model is obtained by scaling down the prototype by a factor λ (while maintaining all the angles unchanged), the model and the prototype are made of the same material (i.e., σ_i and ρ are unchanged), specific impulse due to landmine detonation, *I*, is scaled by a factor λ while pressure due to landmine detonation, P, is kept unchanged, then ε, δ, *a*, and *t* responses of the model are scaled with respect to their prototype counterparts in accordance with the values given in Column 3 of Table 3. When the model is scaled down in accordance with these conditions, then the model is referred to as the *replica-model.*

Table 4 Parameters for defining loading from a landmine

Symbol	Parameter	Fundamental dimensions
P	Pressure due to landmine detonation	F/L^2
I	Specific impulse due to landmine detonation	FT/L^2
E	Landmine detonation-released energy	FL
r	Circular-disk shape landmine thickness	…
r_i	Array of non-thickness (non-dimensional) landmine dimensions	…
d	Landmine depth-of-burial	L
R	Landmine/floor-plate standoff distance	L
P_0	Ambient atmospheric-pressure	F/L^2
a_0	Speed of sound in air	L/T
γ_0	Ratio of specific heats for air	…
ρ	Density of soil	FT^2/L^4
c	Seismic velocity of soil	L/T
g	Gravitational acceleration	L/T^2

2.2.2 Landmine-Detonation-Induced Impulses and Pressures.

Wenzel and Hennessey (Ref 8) also carried a detailed engineering analysis of detonation of landmine shallow-buried in soil. In order to quantify the resulting time-dependant impulses and pressures (input loading parameters in the structural response analysis), they included the effect of the landmine shape and size, type of explosive, soil properties as well as the properties of the surrounding (ambient) air. These parameters along with their fundamental dimensions are listed in Table 4.

Landmine Related Parameters. The landmine was considered to be of a circular-disk shape and to have a size defined by thickness, *r*, and an array of non-dimensional parameters, r_i ($i = 1$, in the present case and r_1 represents thickness-formalized landmine diameter). The type of explosive in the landmine (of a given size) is then expressed by the total energy released during landmine detonation, *E*. The location of the landmine with respect to the model/prototype is defined in terms of the depth-of-burial, *d* (a distance between the top surface of the landmine and the soil/air interface) and standoff distance, *R* (distance between the top surface of the landmine and the bottom of the test plate).

Ambient-Air Parameters. To account for the effects of air blast, three ambient-air parameters are considered: ambient pressure, P_o, sound speed in air, a_0, and a ratio of the constant-pressure and constant-volume specific heats in air, γ_o.

Soil Parameters. To account for the effect of soil (into which the landmine is buried) Wenzel and Hennessey (Ref 8), assumed that detonation of shallow-buried landmine can be related to the problem of underground landmine explosion and the resulting crater formation. Consequently, they assumed that two soil-specific parameters should be included: the (initial) soil density, ρ, and its seismic velocity, *c*. In addition, to include the effect of gravitational forces of the soil surrounding the

Table 5 Π terms for determining loading from landmine

Π term	Physical meaning	Similarity type
$\Pi_1 = r_i$	Array of non-thickness (non-dimensional) landmine dimensions	Geometrical
$\Pi_2 = d/R$	Scaled depth-of-burial	Geometrical
$\Pi_3 = r/R$	Inverse of scaled standoff distance	Geometrical
$\Pi_4 = \gamma_0$	Ratio of specific heats for air	Atmospheric
$\Pi_5 = a_0/c$	Air sound speed to soil seismic speed ratio	Kinematic
$\Pi_6 = P_0R^3/E$	Sach's Number	Ambient
$\Pi_7 = \rho c^2R^3/E$	Modified Sach's Number	Soil
$\Pi_8 = gR/c^2$	Froude Number	Gravitational
$\Pi_9 = PR^3/E$	Non-dimensional pressure due to landmine detonation	Loading
$\Pi_{10} = IcR^2/E$	Non-dimensional impulse due to landmine detonation	Loading

Table 6 Replica-to-prototype scaling for blast-load related parameters

Symbol	Parameter	Scale factor
r, R, d	Circular-disk shape landmine thickness, landmine/floor-plate standoff distance, landmine depth-of-burial	λ
c, a_0	Seismic velocity of soil, speed of sound in air	1.0
γ_0	Ratio of specific heats for air	1.0
ρ	Density of soil	1.0
E	Landmine-detonation-released energy	λ^3
P_0, P	Ambient atmospheric-pressure, pressure due to landmine detonation	1.0
I	Specific impulse due to landmine detonation	λ

landmine, gravitational acceleration, g, is also defined as a physical parameter affecting the temporal evolution of landmine-detonation-induced impulses and pressure.

Resulting Landmine-Detonation Loading Parameters. The discussion presented above introduced 11 landmine, air and soil-related parameters. The remaining two parameters are associated with the landmine-detonation-induced specific impulse, I, and the associated (peak) pressure, P.

Π *Terms.* Three of the parameters listed in Table 4 (i.e., soil density, ρ, soil seismic velocity, c, and the total detonation-released energy, E) are used for non-dimensionalization of the remaining parameters. The resulting 10 Π terms are listed in Table 5.

Scaling. As mentioned earlier, in order for the results obtained using a small-scale model to be applicable to the corresponding full-scale prototype, all Π terms must be maintained unchanged between the small-scale model and the full-scale prototype. The question then arises as to how to scale the landmine/air/soil-related physical parameters listed in Table 4 to achieve this condition. In addition, the scaling for the pressure and for the impulse has already been fixed by the structural-response analysis, Table 3 and this scaling cannot be changed within the present landmine-detonation-analysis.

If r, d and, R are scaled by λ then Π_1 and Π_3 terms are invariant between the model and the prototype. If the same ambient air and soil is used in both the model and the prototype, then Π_4 and Π_5 are invariant. Also, the invariance of the Π_6 and Π_7 terms requires for E to be scaled as λ^3. This is reasonable since all the spatial dimensions are scaled in λ and E depends on the landmine volume.

Since E scales with λ^3 and R scales with λ, then from Π_9 and Π_{10} it is seen that P remains fixed while I is scaled as λ between the model and the prototype. As mentioned earlier, this is exactly the scaling for specific impulse and pressure which was required by the structural-response analysis.

The invariance of the Π_8 term, requires that gravitational acceleration be scaled as $1/\lambda$. In other words, for example, for a one-quarter model, model experiments would have to be done under conditions corresponding to a four times higher gravitational acceleration than the one normally present at the earth. Wenzel and Hennessey (Ref 8) recognized that conducting small-scale experiments under hyper-gravitational conditions would be quite challenging. Consequently, they invoked the study of Westine (Ref 11) which showed that failing to account for the gravitational effects during underground landmine explosion for model in a range between 1/2 and 1/8, resulted in relatively small changes in the resulting crater size. Hence, Wenzel and Hennessey (Ref 8) argued that even though the invariance of the Froude Number (Π_8 term which is defined as a ratio of the gravitational and inertial effects) cannot be generally satisfied, the small-scale model results could be used, with significant confidence, for full-scale prototype design and sizing.

2.2.3 Validation of the Dimensional Analysis. To validate their dimensional analysis presented above, Wenzel and Hennessey (Ref 8) carried out a series of one-half and one-quarter model experiments of floor-plate response to landmine-detonation loads, and compared the results with available full-scale prototype experimental data. They found that the one-half and one-quarter model results (presented in details in section 3) are fully mutually consistent which constituted the proof for validity of the similitude theory they developed. On the other hand, the full-scale results could not be used for dimensional-analyses validation, due to the lack of knowledge of the attendant soil parameters. Nevertheless, the full-scale results revealed that soil parameter play important role in the landmine-detonation-induced loading.

2.3 Computational Problem and Solution Method

The basic formulation of the computational problem dealing with interactions between the detonation products, shell fragments, and soil ejecta (all resulting from the explosion of a shallow-buried landmine) and the target model/prototype hull-bottom plate is presented in this section. All the calculations were carried out using ANSYS/Autodyn (Ref 12), a general purpose transient nonlinear dynamics program. The computational modeling of this interaction involved two distinct steps: (a) geometrical modeling of the model/prototype along with the adjoining mine, air, and soil regions, and (b) the associated transient nonlinear dynamics analysis of the impulse loading (momentum transfer) from the detonation products, shell fragments, and soil ejecta to the target. The part (b) of this analysis was performed using a modified version of the technique developed by Fairlie and Bergeron (Ref 13) which couples a multi-material Eulerian mesh to two Lagrangian meshes. The Eulerian mesh contained initially a Composition-B solid-circular-disk shape buried landmine (and, after explosion, the resulting high-pressure, high-internal energy-density gaseous detonation products) and the (initially stationary, atmospheric-pressure) air (located above the soil). The Eulerian mesh was constructed in terms of eight node cuboidal cells. One of the Lagrangian meshes was used to model the soil, while the other to represent the floor-plate (along with the adjoining hull-supported frame structure). The soil and the target were both discretized using eight-node solid elements (Table 6).

An advantage was taken of the inherent symmetry of the model. In other words, two mutually-orthogonal vertical planes of symmetry were placed along the axis of the target plate as well as along the axis of the air, landmine, and soil regions which enabled only a quarter of the computational model to be analyzed. Representative quarter symmetric models for various computational domains used in the present study are shown in Fig. 2. It should be noted that the lower portion of the Eulerian domain contains the landmine while the rest of the lower portion of the Eulerian domain is occupied by the Lagrangian soil domain. Likewise, the upper portion of the Eulerian domain which extends above the soil contains initially air and is partially occupied by the Lagrangian floor-plate domain.

Air and Composition-B detonation-products are treated as fluids and modeled using only the appropriate equation of state, EOS [i.e., the gamma EOS (Ref 12) for air and the JWL EOS (Ref 12) for Composition-B]. The floor-plate was treated as being made of Rolled Homogenized Armor (RHA) and modeled using a linear equation of state, the Johnson Cook strength and failure models and an instantaneous total equivalent erosion strain algorithm. Details of these models/relations and their parameterizations can be found in Ref 10. Soil was represented using our CU-ARL sand material model (Ref 14-20). The Lagrangian soil elements were allowed to erode at an incremental geometric strain of 2.0. Upon the erosion of an element, the resulting free nodes are allowed to retain their mass/velocity (and, thus, momentum) and to continue to interact with the soil and the target plate.

Interactions between the gaseous fluids (i.e., air and detonation products) with the target plate were accounted for through the use of the appropriate Euler/Lagrange coupling option within ANSYS/Autodyn (Ref 12). Likewise, the soil/target-plate interactions were modeled through the use of the appropriate Lagrange/Lagrange coupling option.

The "flow out" boundary conditions were applied to all the free faces (the faces which do not represent interfaces between the different domains) of the Euler domain except for the face associated with the vertical symmetry planes. To reduce the effect of reflection of the shock waves at the outer surfaces of the Lagrange soil domain, "transmit" boundary conditions were applied to all the free faces of this domain except for the faces associated with the vertical symmetry planes and the upper face which defines the soil/air interface. The transmit boundary conditions enable propagation of the pressure waves across the boundaries without reflection mimicking wave propagation in an infinitely-large soil domain (Ref 12).

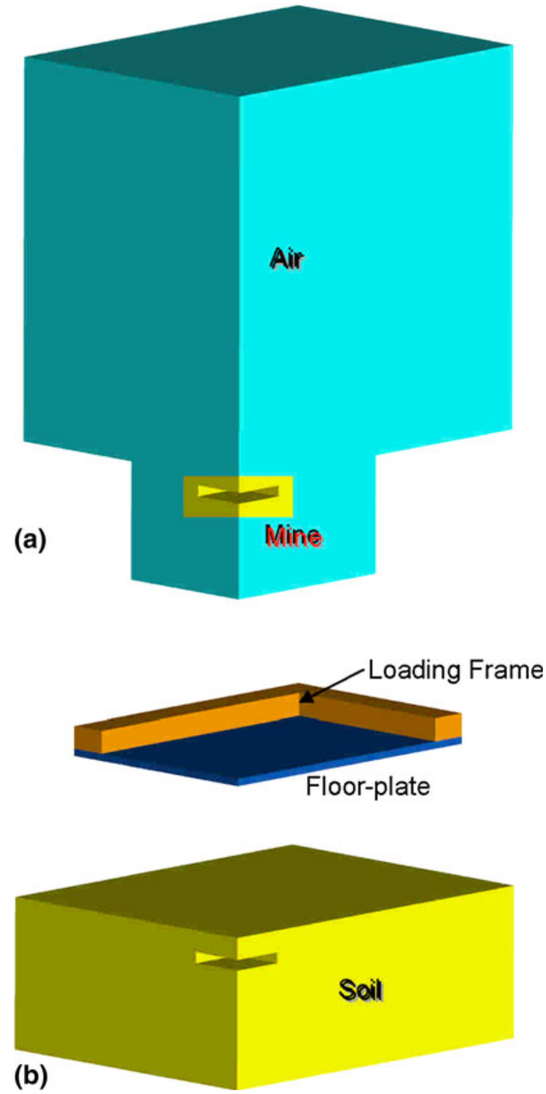

Fig. 2 Computational sub-domains used in the present analysis of structural response of vehicle-hull floor-plate subjected to landmine-blast dynamic loading: (a) Euler sub-domain and (b) Lagrange sub-domain

Several gage points were defined within the landmine, soil, air, and floor-plate which allowed monitoring of the quantities such as pressure, velocity, and (in the case of the Lagrange domains) the vertical displacements.

At the beginning of the simulation, all the Lagrange and Euler domains were activated and the landmine detonated. The (circular-disk shape) landmine was detonated over its entire bottom face at the beginning of the simulation. A standard mesh sensitivity analysis was carried out (the results not shown for brevity) to ensure that the results obtained are not very sensitive to the size of the cells/elements used.

3. Results and Discussion

To comply with the experimental procedure of Wenzel and Hennessey (Ref 8), all the computational analyses carried out in the present work involved a single (full-scale) size of the vehicle-hull floor-plate with $L \times W \times H$ dimensions of 2.13 m by 1.52 m by 0.0254 m. Following the present dimensional analysis, these dimensions were reduced by a factor of 2 and 4 in the case of one-half and one-quarter models, respectively. The initial soil density and its seismic velocity (*sound speed*) were selected to match their experimental counterparts in the work of Wenzel and Hennessey (Ref 8). Also, the same explosive-type (*Composition B*) and floor-plate material (*Rolled Homogenized Armor*, *RHA*) were used to match those used in Ref 8. Initially, two values of the standoff-distance normalized ground clearance (G.C./R) of 0.8889 and 0.8235 (corresponding to ground-clearance values of 14″ = 0.3556 m and 24″ = 0.6096 m, respectively and a fixed/single value of the depth-of-burial of 3″ = 0.0762 m) were selected, in agreement with those used by Wenzel and Hennessey (Ref 8). In order to obtain further insight into the dimensional analysis of landmine-blast induced deformation of the vehicle-hull-floor-plates, additional ground-clearance values were also used in the present computational analyses. The explosive-charge sizes used (at the full scale) at different ground-clearance values are listed in Table 7.

An example of the pressure field in air during detonation of a landmine buried in soil underneath a vehicle-hull floor-plate is shown in Fig. 3. A more detail representation and the discussion of the results obtained in the present work and their experimental counterparts obtained by Wenzel and Hennessey

Table 7 Test matrix pertaining to the selection of explosive-charge sizes, depth-of-burial and floor-plate dimensions at different full-scale ground-clearance levels

	Full-scale ground clearance, m		
Parameter	**0.356**	**0.483**	**0.609**
Composition-B explosive charge, kg	1.81		4.54
	3.18		9.07
	4.54		18.14
	9.07		…
	13.61		…
Depth-of-burial, m	0.076		
Standoff distance, m	0.432	0.559	0.686
Floor-plate, $L \times W \times H$ dimensions, m	2.134 × 1.524 × 0.025		

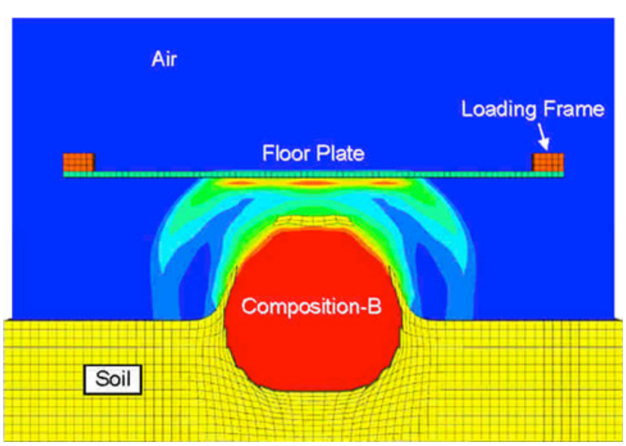

Fig. 3 An example of the air-pressure field during detonation of a mine shallow-buried in soil under a floor-plate target

(Ref 8) is provided in the subsequent sections. It should be recalled that two sets of Π terms were introduced in the present dimensional analysis. One set associated with structural response of the floor-plate while the other corresponding to various aspects of detonation of a landmine buried in soil. To enable clear differentiation between the two sets of Π terms superscripts SR and BL are added to the respective Π terms to denote their structural-response/blast-loading nature.

3.1 Floor-Plate Deflection Versus Explosive-Charge Energy

In this section, the experimental results from Ref 8 and the present computational results pertaining to the dependence of thickness-scaled floor-plate average displacement (Π_4^{SR}, in the structural-response analysis) on the scaled charge energy (Π_7^{BL}, of the detonation-induced impulse/pressure analysis) are presented and discussed.

3.1.1 Examination of the Π_7^{BL} Term as Defined by Wenzel and Hennessey (Ref 8). In Fig. 4(a), the Π_4^{SR} versus Π_7^{BL} results from the work of Wenzel and Hennessey (Ref 8) are presented for the two aforementioned levels of normalized ground clearance. In addition to the measured data points, the corresponding power-law best-fit curves are also shown. The corresponding computational counterpart results obtained in the present work are displayed in Fig. 4(b). Furthermore, to assist an experiment-with-calculation comparison, the best-fit curves from Fig. 4(a) are reproduced in Fig. 4(b). A simple examination/comparison of the results displayed in Fig. 4(a) and (b) reveals that

(a) At each level of the ground clearance, the corresponding full-scale, half-scale, and quarter-scale model computational results are practically identical. This finding suggests that the choice of the two Π terms in Fig. 4(b), was appropriate/justified. Similar conclusion can be drawn based on the experimental results of Wenzel and Hennessey (Ref 8), Fig. 4(a). Nevertheless, it should be noted that all the materials (Composition-B, soil, air and RHA) involved in the present dimensional analysis were kept unchanged. Also, at a given level of scaled ground clearance, Π_7^{BL} value in Fig. 4(a) and (b) was changed by merely changing the value of explosive-charge energy, E (via changing the charge thickness, r). Consequently, it is not clear at this point if the Π_4^{SR} versus Π_7^{BL} relations suggested in Fig. 4(a) and (b) will be valid if properties of the attendant materials and explosive-charge shape are changed. This point will be addressed in greater detail in the remainder of this section.

(b) At each scaled ground-clearance level, the corresponding best-fit curves for the experimental and computational data differ by less than 10%. This finding suggests that there is a reasonably good agreement between the experimental test transient blast-loading conditions used and the floor-plate response observed in the work of Wenzel and Hennessey (Ref 8) and the present transient nonlinear dynamic computational modeling and analysis procedure of the same problem. This finding, and the fact that ground-clearance level is seen to have a significant effect on the Π_4^{SR} versus Π_7^{BL} relationship, suggested the need for additional computational analyses at other values of ground clearance. Since the two aforementioned ground-clearance values of 14 and 24 inches define a fairly realistic range of this quantity in the case

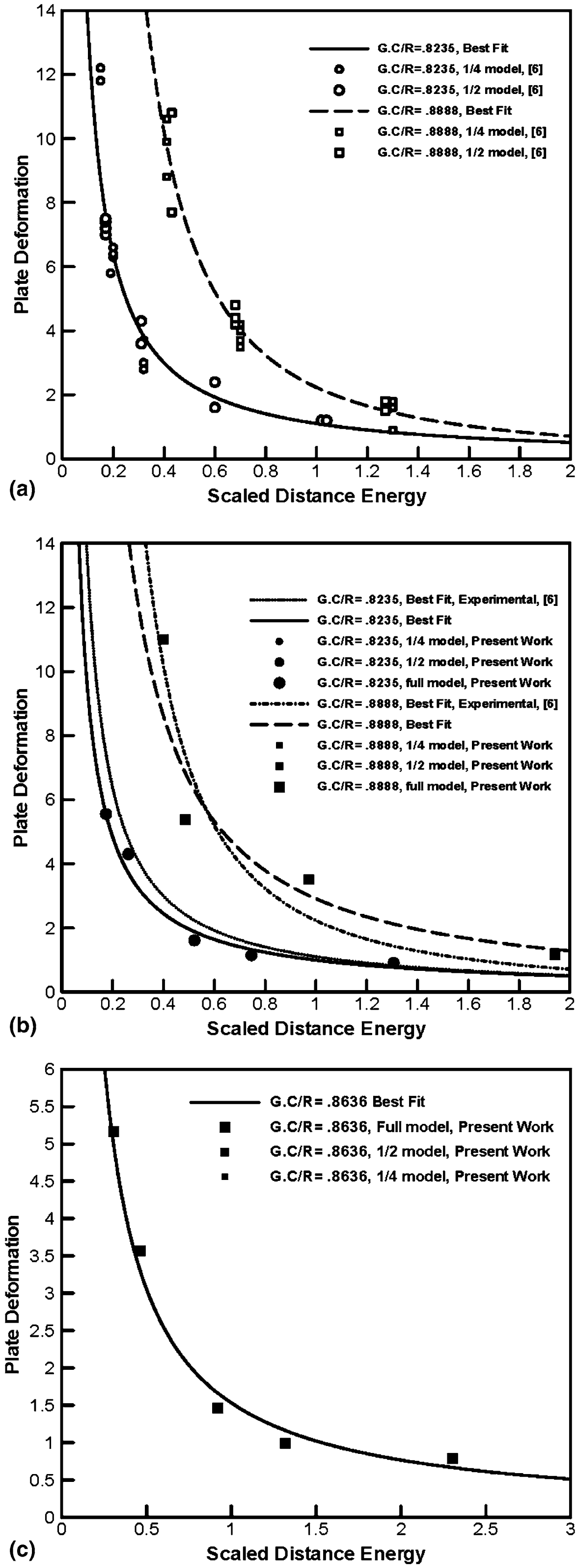

Fig. 4 Variation of the scaled floor-plate deflection with the scaled detonation energy: (a) experimental data from Ref 8 for two scaled ground-clearance levels (0.8235 and 0.8888 m); (b) the corresponding computational results obtained in the present work; and (c) the computational results at an intermediate scaled ground-clearance value of 0.8636 m

of military vehicles, it was decided to add one additional level of ground clearance of 19 inches (corresponding to the normalized ground clearance of 0.8636). The results obtained along with the corresponding power-law best-fit curves are displayed in Fig. 4(c). The results displayed in this figure confirm that choice of the two Π terms for the present dimensional analysis was proper (at least under the conditions of constant explosive, soil, air and floor-plate materials).

The results displayed in Fig. 4(b) and (c) are next used to construct a functional relationship in the form: Π_4^{SR} = function (Π_7^{BL}, Π_2^{BL}), where $\Pi_2^{BL} = 1 - \text{G.C.}/R$ (since $R = \text{G.C.} + d$) and the three standoff-distance normalized values of the ground clearance (G.C./R) were given above. Curve-fitting procedure was next employed using several types of potential functional relationships. Among different candidate formulae, the following function:

$$\Pi_4^{SR} = 1.884(\Pi_7^{BL})^2 - 7.091\Pi_7^{BL} - 34.349\Pi_2^{BL} + 11.897 \quad \text{(Eq 1)}$$

was found to be associated with the highest level of the correlation coefficient.

The results displayed in Fig. 4(a)-(c) suggested that the choice of Π_4^{SR}, Π_7^{BL}, and Π_2^{BL} as the dimensional-analysis Π terms was correct. However, as pointed out earlier, all the experimental tests involving different-scale models were carried out by Wenzel and Hennessey (Ref 8) under constant-soil conditions. Thus, the term ρc^2 in the definition of Π_7^{BL} was not changed. Furthermore, when Wenzel and Hennessey (Ref 8) compared their Π_4^{SR} versus Π_7^{BL} results against full-scale data from other sources (for which the type/condition of soil used was unknown, and potentially different), a highly pronounced disagreement was observed. This finding is examined more closely in the remainder of this section.

The term ρc^2 is, in fact, the bulk modulus which can be described as a measure of the strain energy per unit volume required to double material density under elastic-compression loading conditions. In our previous work (Ref 14-20), it was shown that in the case of saturated soil, volumetric response of the soil surrounding buried explosive charge is indeed dominated by elastic compression (i.e., under high-rate loading conditions, water is mainly trapped in the soil pores and prevents soil particles from moving/sliding). Under these conditions, bulk modulus is a good measure of the energy needed for soil densification. On the other hand, in the case of dry soil, irreversible compaction (i.e., the process of soil-particle sliding, break-up, and compaction) tend to dominate soil response to pressure. Under these conditions, bulk modulus is no longer a good measure of the energy needed for soil compaction. Thus, despite the aforementioned favorable findings related to Fig. 4(a)-(c), the use of the ρc^2 term in the definition of Π_7^{BL} appears troublesome. This contention is further supported by the following simple qualitative argument: First, it should be recognized that the ρc^2 term takes on significantly higher values in the case of saturated soil (since both the initial density and the initial sound speed are higher in saturated- than in the dry-soil case). Hence, in accordance with Fig. 4(a)-(c), this should result in lower values of Π_4^{SR}. However, it is well-established (Ref 14) that saturated soil (due to the fact that it absorbs less detonation energy under compression or shear and that larger volume of saturated soil is ejected during detonation), yield significantly higher impulse values and thus, larger values of floor-plate deflection. Clearly, there will be a problem with the Π_7^{BL} term [as defined by Wenzel and Hennessey (Ref 8)] if it were used across a series of soil types/conditions and that problem is related to the use of ρc^2 in the definition of this Π term. This is further confirmed in Fig. 5(a) in which it is seen that the saturated-soil Π_4^{SR} versus Π_7^{BL} data do not agree with their dry-soil counterparts and that Π_4^{SR} values for the saturated-soil case are considerably higher (as was predicted in our aforementioned argument).

3.1.2 New Definition of the Π_7^{BL} Term. To overcome the aforementioned problem associated with the present dimensional analysis, it is proposed here that Π_7^{BL} term be redefined. Toward that end, the Π_7^{BL} term is first closely examined. The

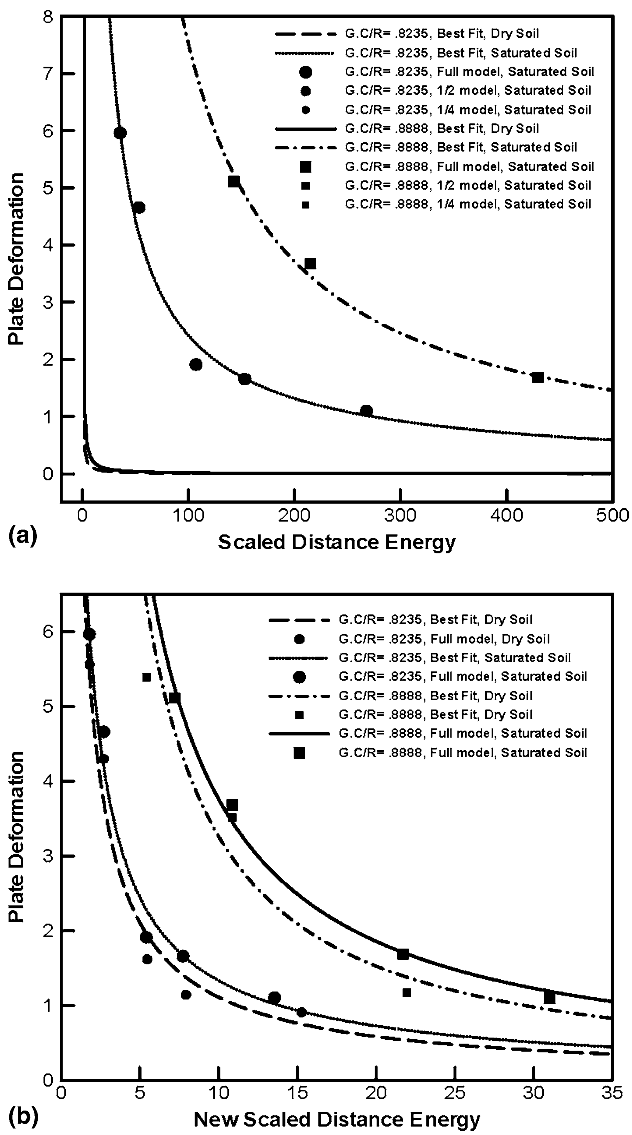

Fig. 5 The effect of soil type (i.e., dry soil vs. saturated soil) on the scaled floor-plate deflection vs. scaled detonation energy (Π_7^{BL}) relationship at two scaled ground-clearance levels (0.8235 and 0.8888 m): (a) original definition of the Π_7^{BL} as proposed by Wenzel and Hennessey (Ref 8) and (b) new definition of the Π_7^{BL}, proposed in the present work

E/R^3 part of this term is simply a statement of the fact that as the detonation-induced spherical shock-wave moves outward from the point of detonation, the average energy density within the spherical domain decreases as $1/R^3$ (the so called Hopkinson rule). To define inverse of the Π_7^{BL} term, Wenzel and Hennessey (Ref 8) divided E/R^3 by ρc^2. However, it was shown above that the use of the ρc^2 term is not fully justified. Also, it should be recognized that not the entire detonation energy, E, should be used in the definition of the Π_7^{BL} but rather its portion, E^*, available after irreversible compaction of soil surrounding the mine has taken place. The energy absorbed by soil during irreversible compaction is a product of the corresponding energy density and the volume of compacted soil. The derivation of simple functional relationships for the compaction energy density and the compacted-soil volume is provided below.

To a first order of approximation, the energy per unit volume associated with full compaction of soil is equal to $e_{comp} = 0.5P_{comp}(\rho_{comp}-\rho_0)/\rho_{comp}$, where P_{comp}, is the overpressure at which full compaction of soil is attained, $\rho_0 = \rho_s(1-\alpha) + \alpha\beta\rho_w$ is the initial zero-overpressure soil density, subscripts s and w are used to denote soil solid-phase and water, respectively while α defines fractional porosity. The degree of saturation, β is defined as a fraction of pores volume filled with water ($\beta = 0.0$, for dry soil and $\beta = 1.0$, for saturated soil). In our previous work (Ref 14-24), it was found that overpressure at which full compaction of soil is attained is a weak function of the degree of saturation. Consequently, this overpressure will be assumed to be constant and set to a value of 650 MPa. Definition of the soil density at full compaction, ρ_{comp} is given by:

$$\rho_{comp} = \left(\frac{1-\alpha}{1-\alpha+\alpha\beta}\right)\rho_s + \left(\frac{\alpha\beta}{1-\alpha+\alpha\beta}\right)\rho_w. \quad \text{(Eq 2)}$$

Under a condition that the volume of detonation-induced irreversibly-compacted-soil is large in comparison with the landmine volume, the soil volume is expected to scale with the third power of a product of the soil seismic velocity and the length of post-detonation time before soil-overburden bubble bursts and rapid discharge of the gaseous detonation-products from the landmine-cavity begins to take place. The soil seismic velocity, c, is a function of the soil porosity, α, and the degree of saturation, β, and the appropriate $c(\alpha,\beta)$ relations were derived in our previous work (Ref 14, 15). It should be noted that c is a material property and, as such, is constant across different model scales. Since the rate of growth of the soil overburden bubble scales with the detonation-energy density, E/R^3, and is thus scale invariant, the post-detonation time at which soil-overburden bubble-burst begins, t_b, is expected to be proportional to the model-scale parameter, λ. Furthermore, in contrast to the soil irreversible-compaction energy density, t_b does not only depend on the soil condition/type, but is also affected by the explosive-charge shape/size and the depth-of-burial. For the fixed values of the depth-of-burial ($d = 0.0762$ m), soil porosity ($\alpha = 0.36$), saturation level ($\beta = 0.0$ and $\beta = 1.0$) and the case of a circular-disk shaped landmine, the full-scale venting-start time t_b dependence on the total detonation-energy E (for the cases of dry soil and saturated soil) is displayed in Fig. 6.

The last part of the Π_7^{BL} term which needs to be modified is the ρc^2 term. This term has the unit of volumetric energy density and, as discussed above, its use is not fully justified. It is our contention, that this should not be any longer related to

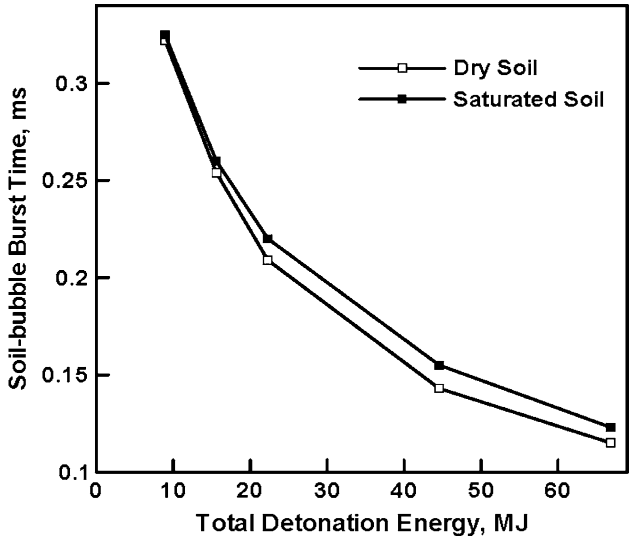

Fig. 6 Variation of the (full-scale) with total detonation energy for dry and saturated soils. The soil-overburden burst time scales directly with the scale factor λ

the soil properties since the main effect of soil associated with detonation-energy absorption has already been included. It is proposed here to use σ term (i.e., the dynamic floor-plate material strength), instead. This term is a measure of the volumetric strain energy density associated with unit plastic-deformation strain. The use of this term appears justified since the early stage of interaction between detonation-products/soil-ejecta and the floor-plate is expected to be dominated by the deformation (and possibly failure) while rigid body motion becomes more pronounced at later stages of the interaction. It should be noted that since Wenzel and Hennessey (Ref 8) and our computational analysis up to this point involve a single RHA material, the σ term is a constant. The effect of different material choice is analyzed later in this section.

With the changes proposed above, the Π_7^{BL} term should be redefined as $\sigma R^3/E^*$ where

$$E^* = E - 4/3\pi c^3 t_b^3 e_{comp}.$$

Using this new definition of the Π_7^{BL} term the results from Fig. 5(a) are recalculated and displayed in Fig. 5(b). Clearly, the agreement between the dry-soil and saturated-soil results is substantially improved suggesting that the new definition of the Π_7^{BL} term (when used across different soil types/conditions) is more appropriate than the definition proposed by Wenzel and Hennessey (Ref 8).

Next, the effect of different floor-plate materials is investigated. The new Π_7^{BL} term suggests that the dominant floor-plate material term is dynamic strength, σ. To check the validity of this assumption two more RHA grades were used whose dynamic strength was obtained by halving and doubling the original yield strength, respectively. Simulations are carried out for both dry and saturated-soil conditions and at two (0.8235 and 0.8888 m) ground-clearance levels. For brevity, only the results pertaining to the case of dry soil are shown in Fig. 7(a) and (b). However, the conclusions reached were based on both sets of results. The results displayed in Fig. 7(a) pertain to the case of the "soft" RHA grade while the ones displayed in Fig. 7(b) pertain to the "hard" RHA grade. A simple examination of the results displayed in these figures suggests

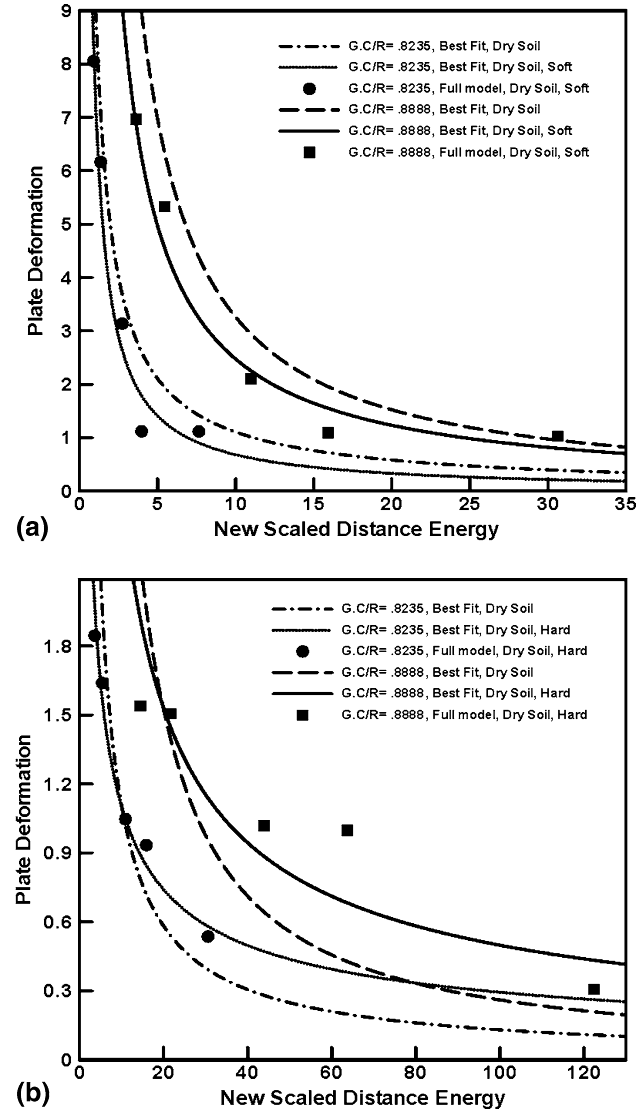

Fig. 7 Variation of the scaled floor-plate deflection with the newly-defined scaled detonation energy for three floor-plate RHA grades: (a) standard and "soft" RHA grades and (b) standard and "hard" RHA grades. The results are obtained computationally for dry soil and two scaled ground-clearance levels (0.8235 and 0.8888 m)

that dynamic strength is one of the major parameters controlling structural response of the floor-plate to landmine-detonation-induced loading. It is, however, not clear if σ is the dominant parameter. Identification of other floor-plate material parameters which may have a significant effect on the floor-plate structural response is beyond the scope of the present work.

3.2 Scaled Floor-Plate Deformation Versus Scaled Response Impulse

The original experimental results from Ref 8 pertaining to the effect of scaled response impulse Π_7^{SR} on the scaled floor-plate deformation Π_4^{SR} are reproduced in Fig. 8(a). In addition, the best-fit curves of these results at two levels of ground clearances used in Ref 8 are shown in the same figure. Also, the corresponding computational results obtained in the present work and their best-fit curves are displayed in Fig. 8(a). A

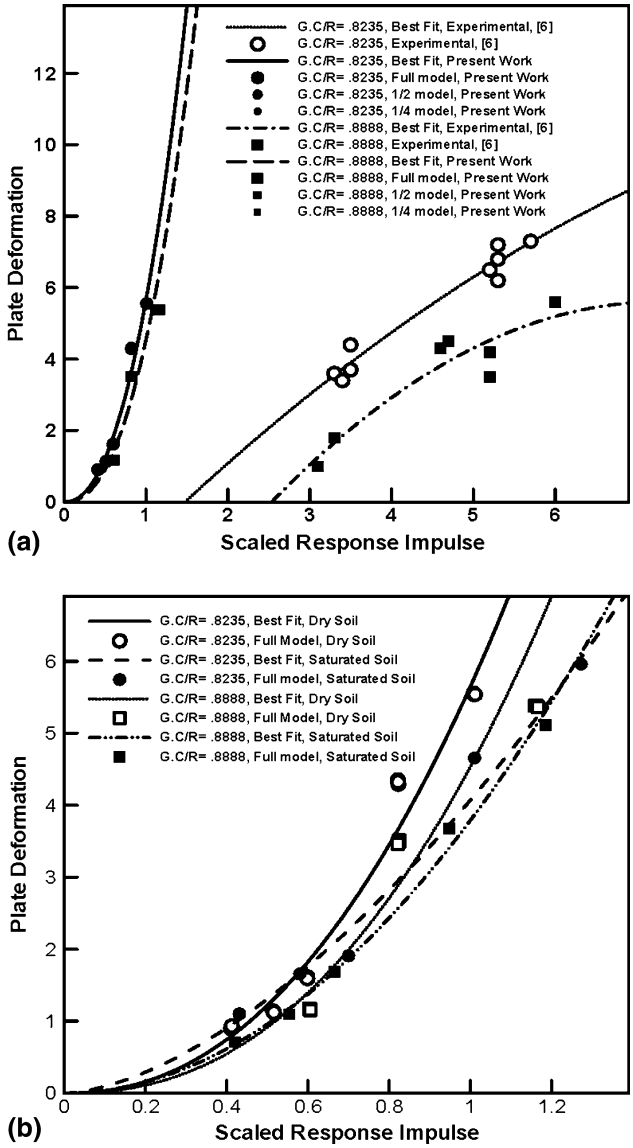

Fig. 8 Variation of the scaled floor-plate deflection with the scaled response impulse for two scaled ground-clearance levels (0.8235 and 0.8888 m): (a) a comparison of the experimental data from Ref 8 and the present computational results for dry-soil and (b) a comparison between dry-soil and saturated-soil computational results

simple examination of the results displayed in Fig. 8(a) reveals that

(a) The corresponding computational results obtained from the full, half, and quarter models are effectively identical suggesting that the choice of the Π_4^{SR} and Π_7^{SR} is appropriate for the present dimensional analysis;

(b) The experimental and computational results are not in a very good agreement. Since the measured and the computed normalized floor-plate deflection data were found to be in good agreement in Fig. 4(b), it is clear that the problem is with the scaled response impulse data. The computed values for this quantity are clearly lower than their experimental counterparts. Since details regarding the technique used by Wenzel and Hennessey to measure the landmine-detonation impulse were not provided in Ref 8, the origin of this discrepancy is not quite clear. However, this discrepancy alone is not sufficient to invalidate the Π term in question.

To provide a more definite answer regarding the validity of the Π_7^{SR} term across different soil condition/types, a comparison between computational Π_4^{SR} versus Π_7^{SR} results for the dry and saturated-soil is provided in Fig. 8(b). This comparison suggests that the choice of Π_7^{SR} as the scaled response impulse was appropriate. While Wenzel and Hennessey (Ref 8) did not provide full justification for the definition of the Π_7^{SR} term, one will be provided here. This Π term can be re-written as:

$$\Pi_4^{SR} = \frac{I}{\sqrt{\rho\sigma xyh}} = \frac{I}{\sqrt{m(\sigma V)}}, \quad \text{(Eq 3)}$$

where $m = \rho V = \rho xyh$ is the floor-plate mass, V the floor-plate volume, and σV is a measure of the strain energy required to deform the floor-plate by unit plastic strain (in the absence of strong strain-hardening effects). The Π_7^{SR} term then is a ratio of the blast-impulse and a product of the inertia-resistance (measured by the floor-plate mass) and the plastic-deformation resistance (as quantified by the σV term).

4. Conclusions

Based on the results obtained in the present work, the following main conclusions can be made:

1. The dimensional analysis for vehicle-hull floor-plate subjected to landmine-detonation loading, originally proposed by Wenzel and Hennessey (Ref 8), has been critically assessed with respect to the physical foundation for the definition of the blast-loading and structural-response Π terms.
2. The results obtained in the present work suggest that, while scaling is proper for all the physical model parameters, a number of Π terms were constructed on a more phenomenological rather than a physical basis. Consequently, the dimensional analysis based on these Π terms provides satisfactory results only under the constraints of constant soil, floor-plate, and ambient-air materials and their conditions.
3. To overcome these limitations of the dimensional analysis of Wenzel and Hennessey (Ref 8), a new definition of one of the key Π terms is proposed based on a detailed investigation of the effect of landmine-detonation gaseous products with the surrounding soil and the accompanying partial absorption of the detonation-released energy. The new definition of the Π terms in question was found to more properly include the effect of soil type/conditions and, to somewhat lesser extent, the effect of floor-plate material properties.

Acknowledgments

The material presented in this paper is based on work supported by the U.S. Army/Clemson University Cooperative Agreements W911NF-04-2-0024 and W911NF-06-2-0042 and by an ARC/TARDEC research contract.

References

1. M. Grujicic, H. Marvi, G. Arakere, W.C. Bell, and I. Haque, The Effect of Up-Armoring the High-Mobility Multi-Purpose Wheeled Vehicle (HMMWV) on the Off-Road Vehicle Performance, *Multidiscip. Model. Mater. Struct.*, 2010, **6**, p 229–256
2. M. Grujicic, G. Arakere, W.C. Bell, and I. Haque, Computational Investigation of the Effect of Up-Armoring on Occupant Injury/Fatality Reduction of a Prototypical High-Mobility Multi-Purpose Wheeled Vehicle Subjected to Mine-Blast, *J. Automob. Eng.*, 2009, **223**, p 903–920
3. M. Grujicic, G. Arakere, H.K. Nallagatla, W.C. Bell, and I. Haque, Computational Investigation of Blast Survivability and Off-Road Performance of an Up-Armored High-Mobility Multi-Purpose Wheeled Vehicle (HMMWV), *J. Automob. Eng.*, 2009, **223**, p 301–325
4. M. Grujicic, W.C. Bell, G. Arakere, and I. Haque, Finite Element Analysis of the Effect of Up-Armoring on the Off-Road Braking and Sharp-Turn Performance of a High-Mobility Multi-purpose Wheeled Vehicle (HMMWV), *J. Automob. Eng.*, 2009, **223**(D11), p 1419–1434
5. M. Grujicic, G. Arakere, T. He, W.C. Bell, P.S. Glomski, and B.A. Cheeseman, Multi-Scale Ballistic Material Modeling of Cross-Plied Compliant Composites, *Compos. B Eng.*, 2009, **40**, p 468–482
6. M. Grujicic, B. Pandurangan, N. Coutris, B.A. Cheeseman, W.N. Roy, and R.R. Skaggs, Computer-Simulations Based Development of a High Strain-Rate, Large-Deformation, High-Pressure Material Model for STANAG 4569 Sandy Gravel, *Soil Dyn. Earthq. Eng.*, 2008, **28**, p 1045–1062
7. M. Grujicic, B. Pandurangan, I. Haque, B.A. Cheeseman, and R.R. Skaggs, A Computational Analysis of Mine Blast Survivability of a Commercial Vehicle Structure, *Multidiscip. Model. Mater. Struct.*, 2007, **3**, p 431–460
8. A. Wenzel and J.M. Hennessey, Analysis and Measurements of the Response of Armor Plates to Land Mine Attacks, *Proceedings of the Army Symposium on Solid Mechanics* (Warren, MI), 1972, p 114–128
9. E. Buckingham, On Physically Similar Systems; Illustrations of the Use of Dimensional Equations, *Phys. Rev.*, 1914, **4**, p 345
10. M. Grujicic, B. Pandurangan, G.M. Mocko, S.T. Hung, B.A. Cheeseman, W.N. Roy, and R.R. Skaggs, A Combined Multi-Material Euler/Lagrange Computational Analysis of Blast Loading Resulting from Detonation of Buried Landmines, *Multidiscip. Model. Mater. Struct.*, 2008, **4**, p 105–124
11. P.S. Westine, Explosive Cratering, *J. Terrramech.*, 1970, **7**(4), p 9–19
12. ANSYS/Autodyn-2D and 3D, *Version 6.1*, *User Documentation*, Century Dynamics Inc., 2006
13. G. Fairlie and D. Bergeron, Numerical Simulation of Mine Blast Loading on Structures, *Proceedings of the 17th Military Aspects of Blast Symposium*, Nevada, June 2002
14. M. Grujicic, B. Pandurangan, and B.A. Cheeseman, The Effect of Degree of Saturation of Sand on Detonation Phenomena Associated with Shallow-Buried and Ground-Laid Mines, *Shock Vib.*, 2006, **13**, p 41–62
15. M. Grujicic, B. Pandurangan, J.D. Summers, B.A. Cheeseman, and W.N. Roy, Application of the Modified Compaction Material Model to Soil with Various Degrees of Water Saturation, *Shock Vib.*, 2008, **15**, p 79–99
16. M. Grujicic, B. Pandurangan, N. Coutris, B.A. Cheeseman, W.N. Roy, and R.R. Skaggs, Derivation and Validation of a Material Model for Clayey Sand for Use in Landmine Detonation Computational Analysis, *Multidiscip. Model. Mater. Struct.*, 2009, **5**, p 311–344
17. M. Grujicic, B. Pandurangan, N. Coutris, B.A. Cheeseman, W.N. Roy, and R.R. Skaggs, Derivation, Parameterization and Validation of a Sandy-Clay Material Model for Use in Landmine Detonation Computational Analyses, *J. Mater. Eng. Perform.*, 2010, **10**, p 434
18. M. Grujicic, B. Pandurangan, Y. Huang, B.A. Cheeseman, W.N. Roy, and R.R. Skaggs, Impulse Loading Resulting from Shallow Buried Explosives in Water-Saturated Sand, *J. Mater. Des. Appl.*, 2007, **221**, p 21–35
19. M. Grujicic, B. Pandurangan, R. Qiao, B.A. Cheeseman, W.N. Roy, R.R. Skaggs, and R. Gupta, Parameterization of the Porous-Material Model for Sand with Different Levels of Water Saturation, *Soil Dyn. Earthq. Eng.*, 2008, **28**, p 20–35
20. M. Grujicic, B. Pandurangan, and B.A. Cheeseman, A Computational Analysis of Detonation of Buried Mines, *Multidiscip. Model. Mater. Struct.*, 2006, **2**, p 363–387
21. M. Grujicic, B. Pandurangan, C.L. Zhao, and B.A. Cheeseman, A Computational Investigation of Various Water-Induced Explosion Mitigation Mechanisms, *Multidiscip. Model. Mater. Struct.*, 2007, **3**, p 185–212
22. M. Grujicic, H. Marvi, G. Arakere, and I. Haque, A Finite Element Analysis of Pneumatic-Tire/Sand Interactions During Off-Road Vehicle Travel, *Multidiscip. Model. Mater. Struct.*, 2010, **6**, p 284–308
23. M. Grujicic and W.C. Bell, A Computational Analysis of Survivability of a Pick-Up Truck Subjected to Mine Detonation Loads, *Multidiscip. Model. Mater. Struct.*, 2011, **7**, p 386–423
24. M. Grujicic, B. Pandurangan, W.C. Bell, and S. Bagheri, Shock-Wave Attenuation and Energy-Dissipation Potential of Granular Materials, *J. Mater. Eng. Perform.*, 2012, **21**, p 167–179